Unsteady Free Convective Flow of a Viscous Incompressible Fluid Past an Exponentially Accelerated Porous Plate with Heat Source

Chinmoy Rath[1,*], Anita Nayak[1]

[1]Department of Mathematics, School of Applied Sciences, Kalinga Institute of Industrial Technology (KIIT) Deemed to be University, Bhubaneswar-751024, Odisha, India.

Abstract:

The problem deals with an unsteady magneto-hydrodynamic natural convective flow of an incompressible viscous radiative fluid past an exponentially accelerated porous plate surrounded by a porous medium with suction or injection and heat source. The novelty of the study is to analyze the impact of different pertinent parameters on the flow due to the presence of heat source in the energy equation. The existence of suction/injection, radiation and heat source in the flow enhances the utility of the research as they are essential in nuclear reactors, thermal and engineering processes etc. The exact solution of the flow equations are obtained using the Laplace transform technique through Bromwich contour. The nature of the flow velocity and temperature profiles due to the impact of pertinent flow parameters are presented graphically. The coefficient of skin friction and rate of heat transfer expressions are obtained analytically, and numerical results through MATLAB are presented in tabular form for various parametric values. It is observed that the insertion of a heat source parameter in the energy equation enhances the velocity of the fluid. The accelerating parameter increases the skin friction coefficient. Nusselt number increases due to fluid suction, whereas fluid injection tends to diminish it. Heat source enhances temperature profiles.

Keywords: Bromwich contour, Heat source, Laplace transform technique, Magnetohydrodynamic (MHD) flow, Suction parameter.

Nomenclature

B: Magnetic field

M: Non-dimensional magnetic field parameter

k': Dimensional permeability of the porous medium

K_p: Non-dimensional permeability of the porous medium

g: Acceleration due to gravity

Gr: Thermal Grashof number

u': Dimensional velocity along x'- direction

u: Non-dimensional velocity along x'- direction

v': Dimensional suction velocity along y'- direction

u_0: Characteristic velocity of the plate

t': Dimensional time

t: Non-dimensional time

a': Dimensional plate acceleration parameter

a: Non-dimensional plate acceleration parameter

a^*: Heat absorption coefficient

C_p: Specific heat of the fluid at constant pressure

D: Mass diffusivity

Nu: Nusselt number

Pr: Prandtl number

q_r: Radiative heat flux

Q_0: Volumetric rate of heat generation

R: Non-dimensional radiation parameter

S: Non-dimensional heat source parameter

T': Dimensional temperature of the fluid

T: Non-dimensional temperature of the fluid

T'_w: Temperature of the plate

T'_∞: Temperature of the fluid at a considerable distance from the plate

Greek Symbols

γ: Non-dimensional suction parameter

μ: Dynamic viscosity of the fluid

ν: Kinematic viscosity of the fluid

ρ: Density of the fluid

β: Volumetric coefficient of thermal expansion

κ: Thermal conductivity of the fluid

σ: Electrical conductivity of the fluid

σ_1: Stefan-Boltzmann constant

τ: Skin friction coefficient

DOI: 10.24297/j.cims.2023.1.9

1. Introduction

Magnetohydrodynamic (MHD) flow occurs in the refinement of crude oil, MHD power generators, aircraft design, the study of plasmas in astrophysics and industrial manufacturing

processes like glass fibre drawing and purification of metals [1]. Fluid flow through porous mediums is observed in water percolation through the soil, osmosis, filtration of pollutants, and dyeing of fabrics in textile industries. A detailed description of convection via a porous medium is given in the book by Nield and Bejan [2]. Many researchers have studied the MHD flow occurring past porous surfaces. Shawky *et al.* [3] have investigated the MHD flow of Williamson nanofluid past an extending porous sheet. Their findings reported an enhanced fluid flow with permeability parameter. The study of the effect of radiation and chemical reaction on the MHD flow of Maxwell nanofluid past a porous medium was done by Reddy and Lakshminarayana [4]. Fluid suction is a technique by which the formation of the boundary layer is controlled while delaying the transition from laminar to turbulent flow. Pattnaik *et al.* [5] conducted a study of the impact of thermal radiation on the MHD flow past an exponentially accelerated inclined plate. The effect of suction was not included in their model. The consequence of plate temperature and concentration growing at an exponential rate on MHD flow occurring past a permeable plate in the absence of suction was investigated by Umamaheswar *et al.* [6]. Paul [7] has obtained an exact analytical solution of MHD flow, depending on time, with fluid suction influenced by thermal radiation via Laplace transform technique. The author concluded that the convective heat transfer rate near the plate got a boost with radiation and suction.

The study of the flow of fluids in the presence of internal heat generation or absorption is essential as such flows are prevalent in the cooling of nuclear reactors, refrigerators and endothermic and exothermic chemical reactions. Ajibade *et al.* [8] obtained a semi-analytical solution to the problem of MHD flow in the presence of suction/injection and internal heat generation/absorption. The investigation of the impact of radiation and heat source on the time-dependent MHD flow through a porous channel was done by Makinde *et al.* [9]. The investigation revealed that the heat source gave a boost to the rate of convective heat transfer at the porous walls. Reddy *et al.* [10] have studied the impact of heat source and dissipation of heat on the MHD convective flow occurring along an exponentially stretching sheet. The effect of heat source on the MHD flow of micropolar fluid was studied by Bejawada *et al.* [11].

The current research investigates the impact of suction/injection and heat source on the unsteady magnetohydrodynamic viscous, radiative fluid flowing past an exponentially accelerated vertical permeable plate enveloped by a porous medium. We have extended the work of Paul [7] by considering a heat source with suction/blowing. For a more accurate result, an exact closed-form solution of the governing equations was obtained with the help of the

Laplace transform technique through Bromwich contour integration manually for unit Prandtl number. The results are presented graphically through MATLAB, and the variation of skin friction and Nusselt number with multiple values of the parameters are exhibited via table. A comparison of the present work with Paul [7] was made in Fig. 12, and the results are in good agreement with Paul [7].

2. Mathematical Formulation

We have considered a time-dependent magnetohydrodynamic free convective flow along a vertical plate in the present work. The fluid is incompressible, viscous and radiating. The x'- axis is considered along the vertical plate and y'- axis is taken transverse to the plate. The model considers the plate, as well as the medium, to be porous. The flow is two-dimensional, meaning there is no flow and variation of flow variables along z'- direction. The plate extends along the x'- direction. It is understood that all the variables of the problem are functions of y' and t' only except pressure. A transverse magnetic field $\vec{B} = (0, B_0)$ having uniform intensity B_0 acts parallel to the y'- axis.

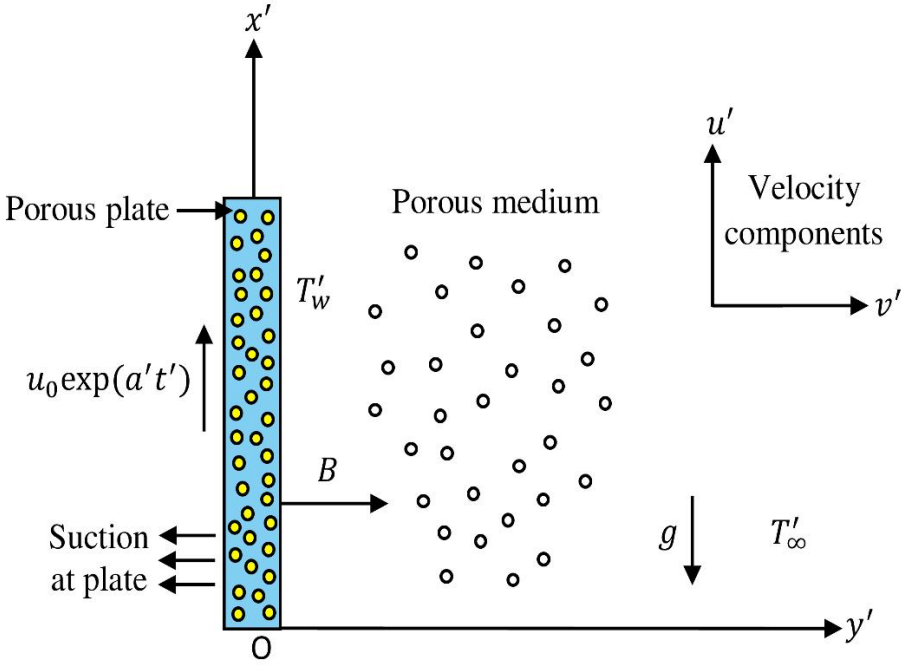

Fig. 1. The model of the problem.

A constant suction operating at the porous plate along y' - direction is considered. In the beginning, for $t' \leq 0$, both the plate and the surrounding fluid are static with temperature T'_∞. From time $t' = 0$ onwards, the motion of the plate occurs in the $x'y'$ - plane with a velocity of $u_0 \exp(a't')$. The temperature of the plate boundary varies linearly with time t'. The induced

magnetic field effects are neglected due to the low magnetic Reynolds number of the flow regime [12]. The Ohm' s law for conducting fluids gives us

$$\vec{J} = \sigma\left(\vec{u}X\ \vec{B}\right)\#(1)$$

From Eq. (1), we get the Lorentz force per unit volume of the fluid as

$$\overrightarrow{F_{Lorentz}} = (-\sigma B_0^2 u', 0)\#(2)$$

Following Schlichting and Gersten [13] and Paul [7], the unsteady governing equations of the present problem are:

$$\frac{\partial v'}{\partial y'} = 0\#(3)$$

$$\frac{\partial u'}{\partial t'} + v'\frac{\partial u'}{\partial y'} = \nu\frac{\partial^2 u'}{\partial y'^2} + g\beta\left(T' - T'_\infty\right) - \frac{\sigma B_0^2}{\rho}u' - \frac{\nu}{k'}u'\#(4)$$

$$\rho C_p\left[\frac{\partial T'}{\partial t'} + v'\frac{\partial T'}{\partial y'}\right] = \kappa\frac{\partial^2 T'}{\partial y'^2} - \frac{\partial q_r}{\partial y'} + Q_0\left(T' - T'_\infty\right)\#(5)$$

The initial and boundary conditions of the problem are:

$$t' \le 0: u' = 0;\ T' = T'_\infty\ for\ all\ y'$$

$$t' > 0: u' = u_0\exp\left(a't'\right);\ T' = T'_\infty + \left(T'_w - T'_\infty\right)\frac{u_0^2 t'}{\nu}\ at\ y' = 0$$

$$t' > 0: u' \to 0;\ T' \to T'_\infty\ as\ y' \to \infty \quad (6)$$

The fluid is assumed to be optically thin, grey, heat-absorbing or heat-emitting ([5,7]). The fluid scatters no heat. The expression for the local gradient of the radiative heat flux is

$$\frac{\partial q_r}{\partial y'} = -4a^*\sigma_1\left(T'^4_\infty - T'^4\right)\#(7)$$

with a^* and σ_1 being the absorption coefficient and the Stefan-Boltzmann constant, respectively. T'^4 is expressed as a linear function of T' by assuming that the temperature variation $T' - T'_\infty$ is sufficiently small. Omitting the higher-order terms in Taylor' s expansion of T'^4 about T'_∞, we obtain the expression

$$T'^4 = 4T'^3_\infty T' - 3T'^4_\infty\ \#(8)$$

Using Eq. (8) in Eq. (7), the energy equation Eq. (5) is rewritten as

$$\rho C_p\left[\frac{\partial T'}{\partial t'} + v'\frac{\partial T'}{\partial y'}\right] = \kappa\frac{\partial^2 T'}{\partial y'^2} + 16a^*\sigma_1 T'^3_\infty\left(T'_\infty - T'\right) + Q_0\left(T' - T'_\infty\right)\#(9)$$

The non-dimensional variables are defined as follows:

$$u = \frac{u'}{u_0}, y = \frac{y'u_0}{\nu}, t = \frac{t'u_0^2}{\nu}, T = \frac{T' - T'_\infty}{T'_w - T'_\infty},$$

$$Pr = \frac{\mu C_p}{\kappa}, Gr = \frac{g\beta\nu(T'_w - T'_\infty)}{u_0^3}, M = \frac{\sigma B_0^2\nu}{\rho u_0^2}, K_p = \frac{k'u_0^2}{\nu^2},$$

$$R = \frac{16a^*\nu^2\sigma_1 T'^3_\infty}{\kappa u_0^2}, S = \frac{Q_0\nu}{\rho C_p u_0^2}, a = \frac{a'\nu}{u_0^2}, \gamma = -\frac{v'}{u_0}\#(10)$$

After non-dimensionalization, the governing equations take the form:

$$\frac{\partial u}{\partial t} - \gamma\frac{\partial u}{\partial y} = \frac{\partial^2 u}{\partial y^2} + GrT - Mu - \frac{u}{K_p}\ \#(11)$$

$$\frac{\partial T}{\partial t}-\gamma\frac{\partial T}{\partial y}=\frac{1}{Pr}\frac{\partial^2 T}{\partial y^2}-\frac{R}{Pr}T+ST\#(12)$$

subject to the non-dimensionalized initial and boundary conditions:

$$\begin{aligned}&t\le 0: u=0;\ T=0\ for\ all\ y\\&t>0: u=\exp(at);\ T=t\ at\ y=0\\&t>0: u\to 0;\ T\to 0\ as\ y\to\infty\end{aligned}\qquad(13)$$

3. Analytical Method Of Solution

An exact solution of the above system of partial differential equations by Laplace transform through Bromwich contour has been obtained for unit Prandtl number manually analyzing Paul and Deka [14] and Deka *et al.* [15]. Applying the Laplace transform technique to Eqs. (11)–(12) under the boundary conditions (13), the results for velocity and temperature are:

$$\overline{u}=\frac{\exp\left(-\left(\frac{\gamma}{2}+\sqrt{s+F_1}\right)y\right)}{s-a}+\frac{Gr\exp\left(-\left(\frac{\gamma}{2}+\sqrt{s+F_1}\right)y\right)}{\alpha_1 s^2}-\frac{Gr\exp\left(-\left(\frac{\gamma}{2}+\sqrt{s+F_2}\right)y\right)}{\alpha_1 s^2}\ \#(14)$$

$$\overline{T}=\frac{\exp\left(-\left(\frac{\gamma}{2}+\sqrt{s+F_2}\right)y\right)}{s^2}\ \#(15)$$

where $\overline{u},\overline{T}$ are the Laplace transforms of u,T respectively, with $s>0$ being the Laplace transform variable. Using the Bromwich contour integration, the inverse Laplace Transform of a function $F(s)$ is given as

$$L^{-1}[F(s)]=\frac{1}{2\pi i}\int_{Br_1}\exp(st)\,F(s)\,ds\ \#(16)$$

where Br_1 is the first Bromwich contour joining the points $c-i\infty$ to $c+i\infty$ with c chosen such that all the singularities of $F(s)$ lie to the left of Br_1. The occurrence of square root terms as arguments of the exponential function make it challenging to integrate along Br_1. Thus we use the quadratic transformation $s=\xi^2$ to transform into an equivalent contour Br_3 defined by McLachlan [16]. The inverse Laplace Transform of Eqs. (14)–(15) following [16] is given as:

$$\frac{1}{2\pi i}\int_{Br_3}\frac{\exp(\xi^2 t-b\xi)}{\xi\pm a}\,d\xi=\frac{\exp(a^2t\pm ab)}{2}erfc\left(\frac{b\pm 2at}{2\sqrt{t}}\right)\ \#(17)$$

$$\frac{1}{\pi i}\int_{Br_3}\frac{\exp\left(\frac{\xi^2 t}{a}-y\xi\right)}{\left(\xi\pm\sqrt{ab}\right)^2}\,d\xi=2\sqrt{\frac{t}{a\pi}}\exp\left(-\frac{ay^2}{4t}\right)\mp\left(\frac{2t\sqrt{ab}}{a}\pm y\right)\exp\left(bt\pm y\sqrt{ab}\right)erfc\left(\frac{y}{2}\sqrt{\frac{a}{t}}\pm\sqrt{bt}\right)\ \#(18)$$

where a,b are constants, and $erfc$ is the complementary error function. Hence, the exact solution for velocity and temperature equations are:

$$u=\frac{\exp\left(-\frac{\gamma y}{2}\right)}{2}\left[\begin{array}{l}\exp(at)\left\{\begin{array}{l}\exp\left(y\sqrt{a+F_1}\right)erfc\left(\frac{y}{2\sqrt{t}}+\sqrt{(a+F_1)t}\right)\\+\exp\left(-y\sqrt{a+F_1}\right)erfc\left(\frac{y}{2\sqrt{t}}-\sqrt{(a+F_1)t}\right)\end{array}\right\}\\+\frac{Gr}{\alpha_1}\left\{\begin{array}{l}\left(t+\frac{y}{2\sqrt{F_1}}\right)\exp\left(y\sqrt{F_1}\right)erfc\left(\frac{y}{2\sqrt{t}}+\sqrt{F_1t}\right)\\+\left(t-\frac{y}{2\sqrt{F_1}}\right)\exp\left(-y\sqrt{F_1}\right)erfc\left(\frac{y}{2\sqrt{t}}-\sqrt{F_1t}\right)\end{array}\right\}\\-\frac{Gr}{\alpha_1}\left\{\begin{array}{l}\left(t+\frac{y}{2\sqrt{F_2}}\right)\exp\left(y\sqrt{F_2}\right)erfc\left(\frac{y}{2\sqrt{t}}+\sqrt{F_2t}\right)\\+\left(t-\frac{y}{2\sqrt{F_2}}\right)\exp\left(-y\sqrt{F_2}\right)erfc\left(\frac{y}{2\sqrt{t}}-\sqrt{F_2t}\right)\end{array}\right\}\end{array}\right] \#(19)$$

$$T=\frac{\exp\left(-\frac{\gamma y}{2}\right)}{2}\left[\begin{array}{l}\left(t+\frac{y}{2\sqrt{F_2}}\right)\exp\left(y\sqrt{F_2}\right)erfc\left(\frac{y}{2\sqrt{t}}+\sqrt{F_2t}\right)\\+\left(t-\frac{y}{2\sqrt{F_2}}\right)\exp\left(-y\sqrt{F_2}\right)erfc\left(\frac{y}{2\sqrt{t}}-\sqrt{F_2t}\right)\end{array}\right] \#(20)$$

Skin friction coefficient

The non-dimensional expression for the skin friction coefficient is

$$\tau=-\left.\frac{\partial u}{\partial y}\right|_{y=0} \#(21)$$

From Eq. (19), the computed expression of the skin friction coefficient is:

$$\begin{aligned}\tau=\frac{\gamma}{2}\exp(at)+\exp(at)\left\{\sqrt{a+F_1}\left(1-erfc\left(\sqrt{(a+F_1)t}\right)\right)+\frac{1}{\sqrt{\pi t}}\exp\left(-(a+F_1)t\right)\right\}\\+\frac{Gr}{\alpha_1}\left\{\left(\frac{1}{2\sqrt{F_1}}+t\sqrt{F_1}\right)\left(1-erfc\left(\sqrt{F_1t}\right)\right)+\sqrt{\frac{t}{\pi}}\exp\left(-F_1t\right)\right\}\\-\frac{Gr}{\alpha_1}\left\{\left(\frac{1}{2\sqrt{F_2}}+t\sqrt{F_2}\right)\left(1-erfc\left(\sqrt{F_2t}\right)\right)+\sqrt{\frac{t}{\pi}}\exp\left(-F_2t\right)\right\} \#(22)\end{aligned}$$

Nusselt number

The non-dimensional expression for the Nusselt number can be written as

$$Nu=-\left.\frac{\partial T}{\partial y}\right|_{y=0} \#(23)$$

From Eq. (20), the expression for the Nusselt number is derived as:

$$Nu=\frac{\gamma t}{2}+\left(\frac{1}{2\sqrt{F_2}}+t\sqrt{F_2}\right)\left(1-erfc\left(\sqrt{F_2t}\right)\right)+\sqrt{\frac{t}{\pi}}\exp\left(-F_2t\right) \#(24)$$

where $\lambda=M+1/K_p$, $F_1=\gamma^2/4+\lambda$, $F_2=\gamma^2/4+R-S$, $\alpha_1=R-S-\lambda$.

4. Results And Discussions

In the present analysis, the governing equations of the problem have been solved exactly by applying the Laplace transform technique for unit Prandtl number. For general Prandtl number

in the existence of suction, the computation of inverse Laplace transformation becomes too complicated and difficult to solve for a coupled system of differential equations. The physics of velocity and temperature are discussed through graphs and are plotted using MATLAB. Tabular values are obtained for skin friction coefficient and Nusselt number. The default values of the parameters considered in the computation are $Gr = 3, M = 0.7, K_p = 0.3, R = 6, S = 5, t = 0.6, a = 0.8$ and $\gamma = 0.9$.

Velocity profile

Fig. 2 represents the impact of the Grashof number on the profiles of velocity. It is understood that enhancing the value of QUOTE Gr Gr (cooling of the plate) acts as a booster for the velocity of the fluid as expected. Increasing the Grashof number results in a more significant buoyancy force, which accelerates the fluid particles and fluid velocity, for which there is an increase in boundary layer thickness. The reverse effect is observed in the case of $Gr < 0$. The physics behind $(Gr < 0)$ represents heating of the boundary (cooling of the fluid), $(Gr > 0)$ signifies cooling of the boundary (heating of the fluid) and $(Gr = 0)$ represents no natural convection current. Thus, heating and cooling show contradictory buoyancy effects. Fig. 3 displays the impact of the magnetic parameter QUOTE M, on the velocity profiles. It is discovered that velocity declines with a higher magnetic field. This is due to the fact that the Lorentz force resists the motion of the fluid particles for which the velocity profiles decrease. Fig. 4 portrays the impact of the permeability parameter on the profiles of velocity. It is seen that velocity profiles increase with a larger value of the permeability parameter. Fig. 5 verifies the degradation of velocity profiles due to radiation parameter. Because of radiation, additional heat is generated, for which more drag force is produced. As a result, the fluid velocity decelerates as expected. Fig. 6 defines the influence of heat source parameter on the profiles of velocity. It reveals that the velocity profiles enhance with increasing heat source parameter values. Thus, it indicates that the presence of heat source in the energy equation is favourable to increasing the velocity of the fluid. It is noticeable because when heat is absorbed, the buoyancy force increases, and the rate of heat flow increases, for which the velocity of the fluid increases. In contrast, a heat sink acts in the opposite way towards the development of velocity. The impact of accelerating parameter QUOTE a a on velocity profiles can be discerned in Fig. 7. There is evidence that the accelerating parameter enhances fluid velocity, which is evident from the figure and when QUOTE > 1 $y > 1$, the velocity attains a steady state. This is the property of the parameter of an exponentially accelerated vertical plate. Fig. 8 exhibits the impact of suction/injection on the profiles of velocity. It is seen that for higher values of suction QUOTE $(\gamma > 0$ $(\gamma > 0)$, the velocity of the fluid

reduces, whereas the reverse effect is observed in the case of injection (QUOTE $\gamma < 0$) $\gamma < 0$). It is also observed that the boundary layer thickness is smaller in the case of suction in comparison to injection.

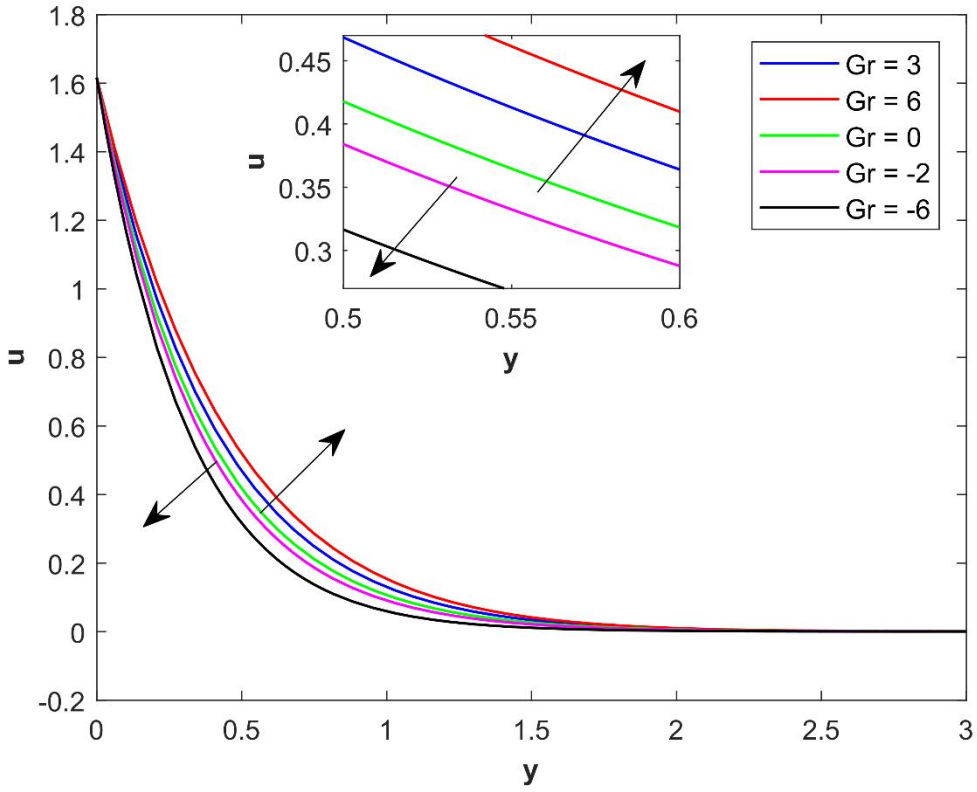

Fig. 2. The variation of velocity $\boldsymbol{u}$ with $\boldsymbol{Gr}$.

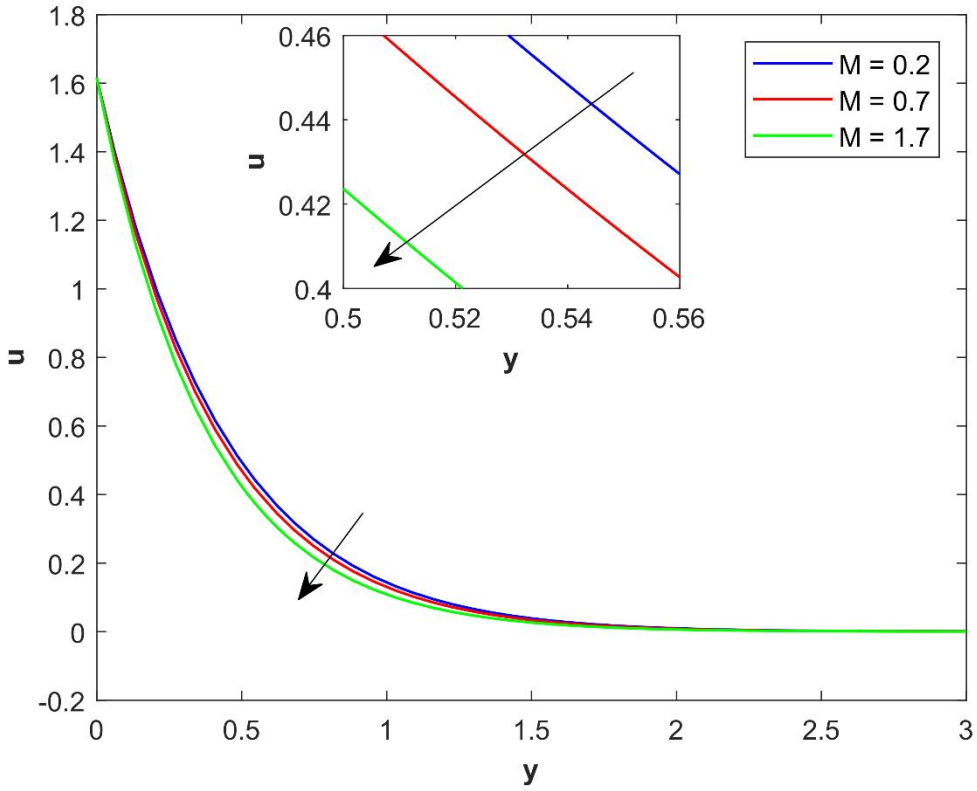

Fig. 3. The variation of velocity u with

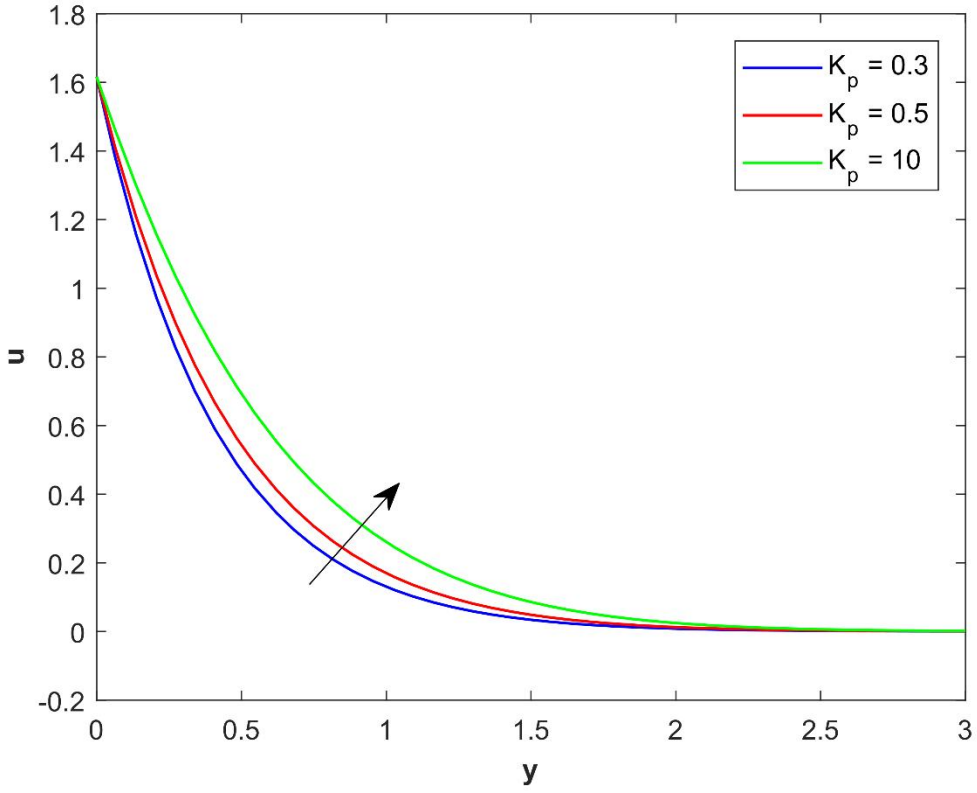

M.

Fig. 4. The variation of velocity u with K_p.

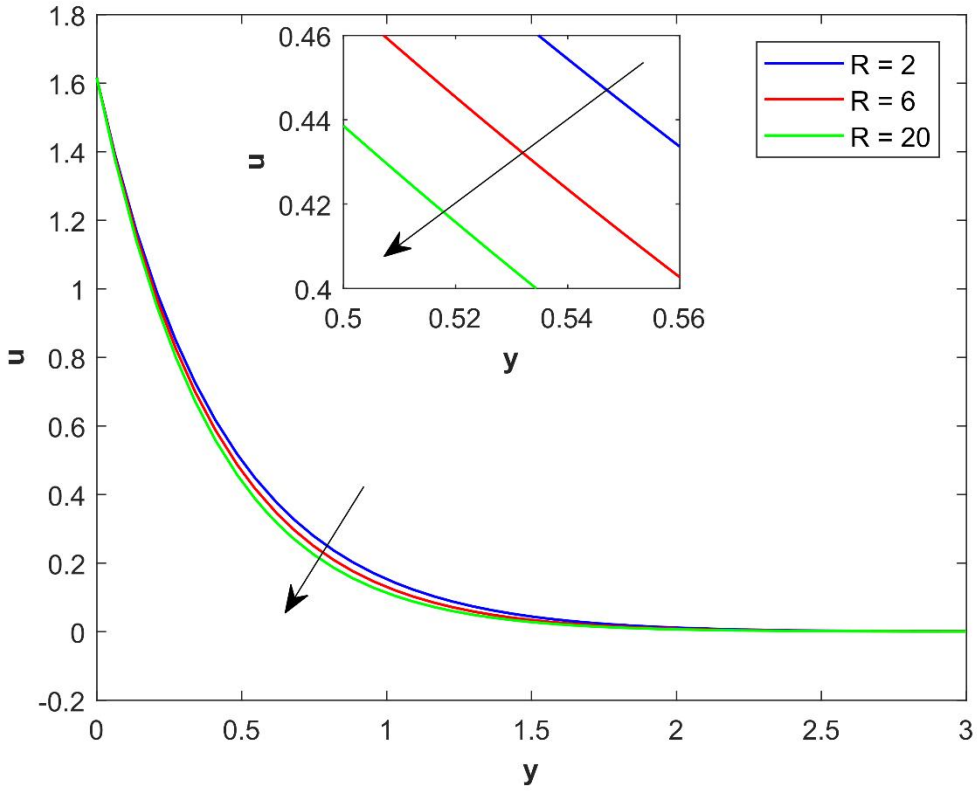

Fig. 5. The variation of velocity u with

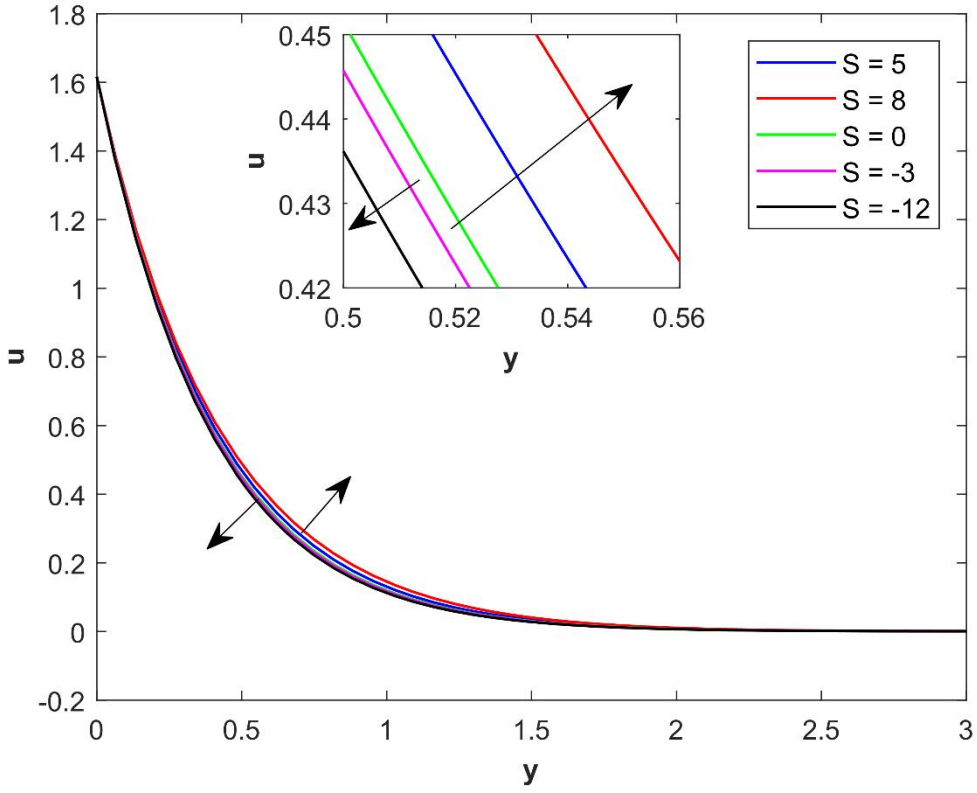

R.

Fig. 6. The variation of velocity u with S.

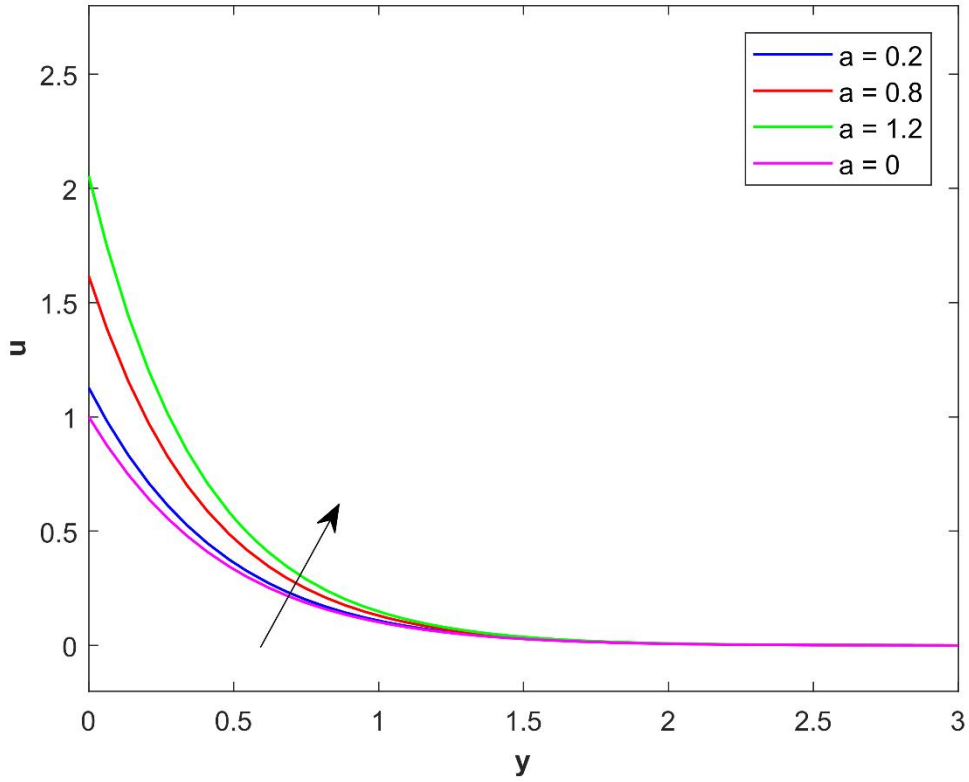

Fig. 7. The variation of velocity u with a.

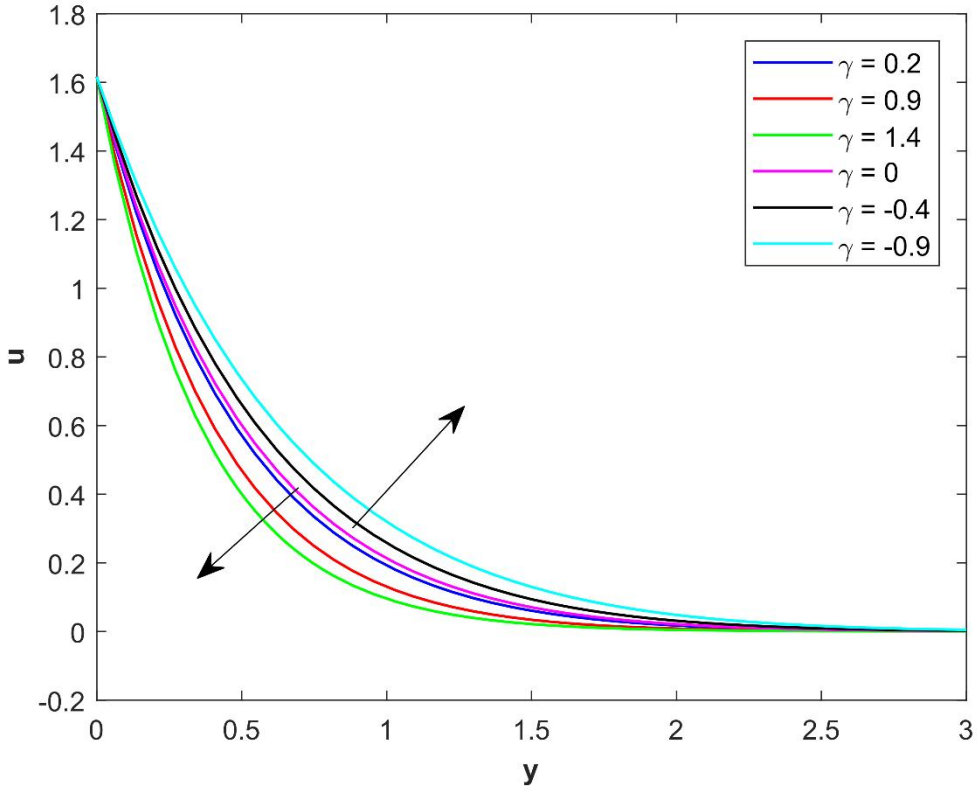

Fig. 8. The variation of velocity u with γ.

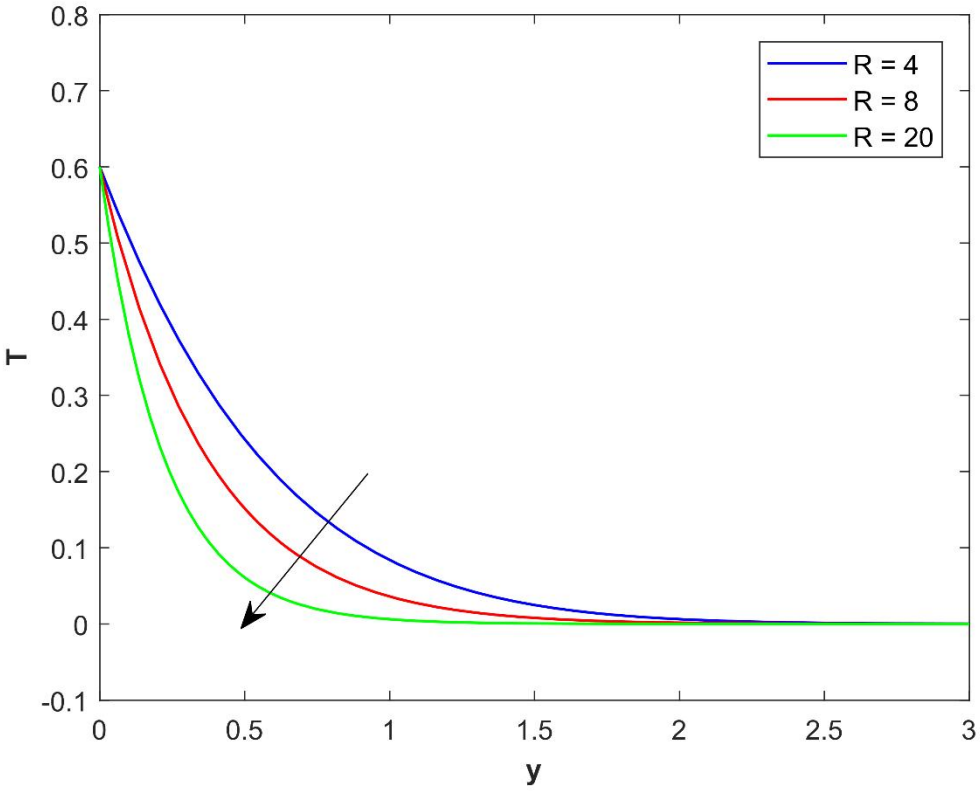

Fig. 9. The variation of temperature T with

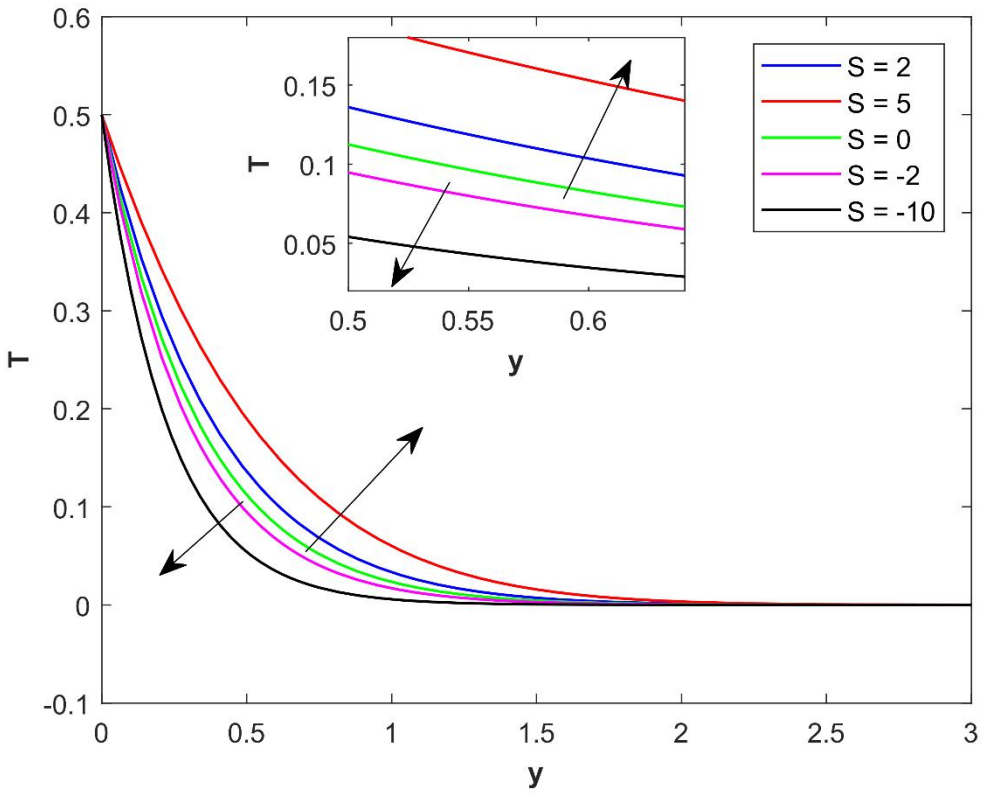

R.

Fig. 10. The variation of temperature T with S.

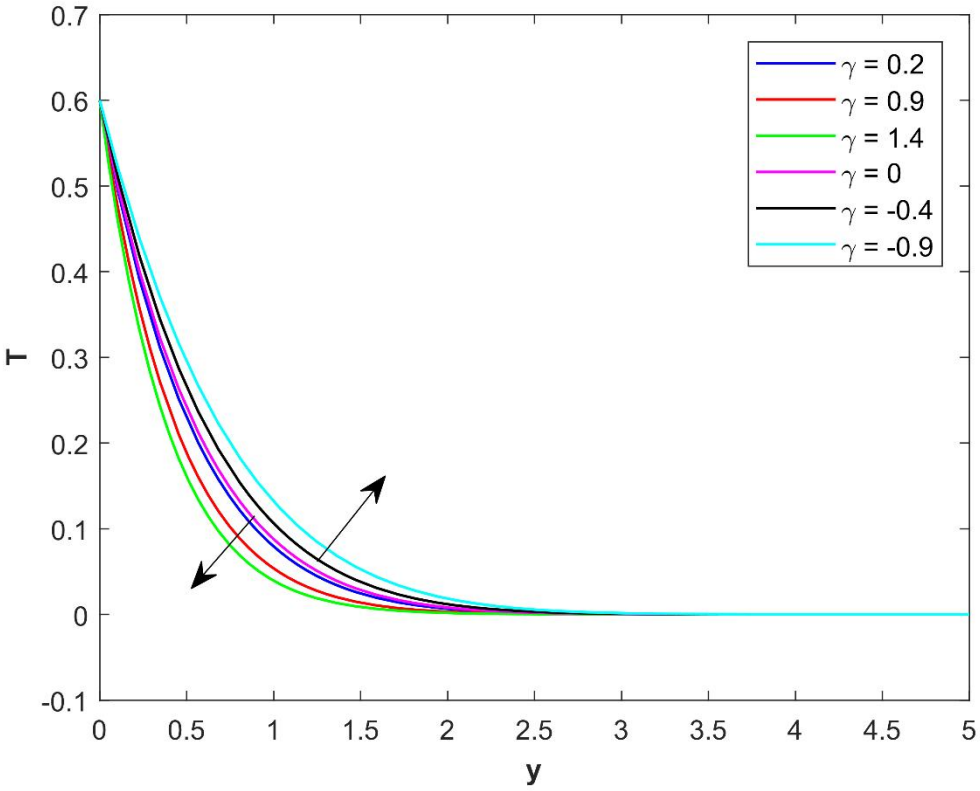

Fig. 11. The variation of temperature T with γ.

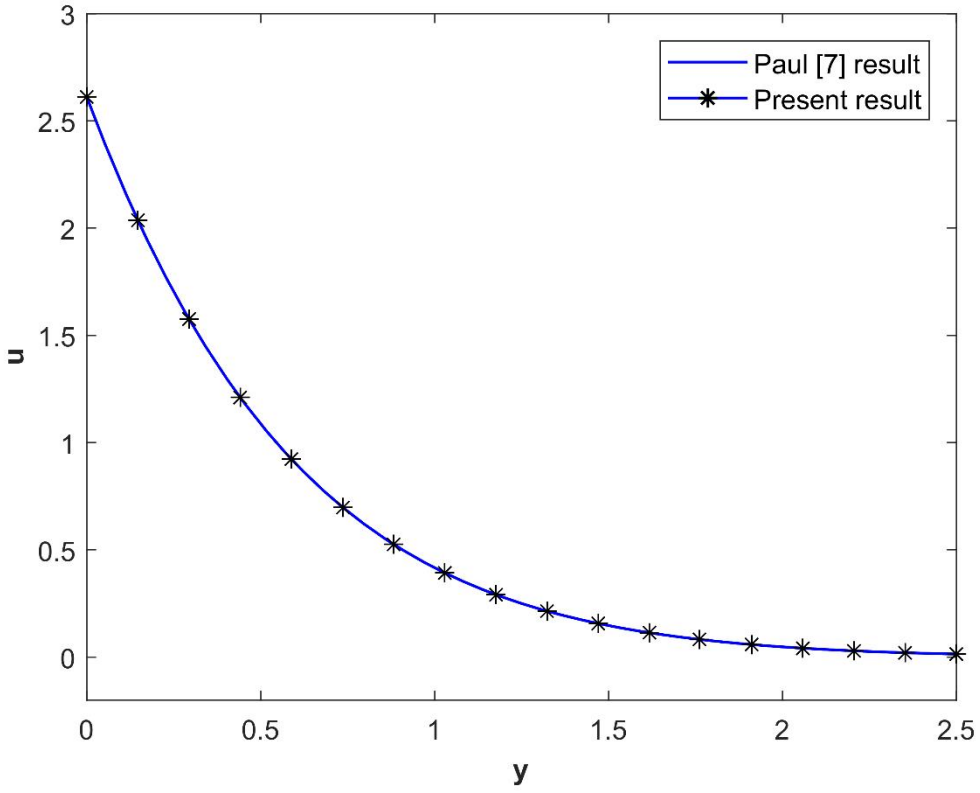

Fig. 12. A comparison of velocity profiles with Paul [7].

Temperature profile

Fig. 9 represents the effect of the radiation parameter QUOTE (R) (R) on the profiles of temperature. It is clear that the thermal state of the fluid weakens with an escalation of radiation. This is because in the case of gases QUOTE $(Pr = 1)$, $(Pr = 1)$, an increased value of QUOTE R, R, lowers the heat flow as well as fluid temperature. Fig. 10 indicates the influence of heat source parameter on temperature profiles. It is revealed that the heat source acts as a booster for profiles of temperature. The reason is that thermal energy, in addition to the kinetic energy of the fluid, shoots up as a stronger heat source is applied. The temperature falls when a heat sink is applied to the system. The effect of suction/injection on temperature profiles is presented in Fig. 11. It is seen that temperature for a higher value of injection QUOTE $(\gamma < 0)$ $(\gamma < 0)$ increases, whereas the reverse effect is observed in the case of suction QUOTE $(\gamma > 0)$ $(\gamma > 0)$. The conclusions obtained here agree with Paul [7], representing a thicker thermal boundary layer subject to conversion from suction to injection.

Skin friction coefficient and Rate of heat transfer

Table 1 represents the skin friction coefficient and rate of heat transfer for different values of the pertinent parameters. The coefficient of skin friction gets improved with higher values of M, R, a and γ, while it gets reduced with increasing values of Gr, K_p and S. The increase in skin friction is pronounced when the plate is accelerated to a greater extent. This happens because the fluid viscosity tends to retard the accelerated motion and the skin friction drag increases. A stronger magnetic field boosts the skin friction coefficient, whereas increased permeability of the medium declines it. The skin friction decreases with the heat source while it increases with the heat sink parameter. Fluid suction enhances skin friction, whereas fluid injection tends to diminish it. It is also observed that injection and internal heat generation diminish the rate of heat transfer near the plate, and on the other hand, suction, radiation and internal heat absorption act as a booster to it. The current result agrees well with that of Paul [7].

5. Validation

For validation, a portion of Fig. 6 of Paul [7] is reproduced in Fig. 12. The values of the parameters are taken as QUOTE $Gr = 8, M = 1, K_p = 0.5, t = 0.8, R = 2, a = 1.2$ $Gr = 8, M = 1, K_p = 0.5, t = 0.8, R = 2, a = 1.2$ and QUOTE $= 0.4$ $\gamma = 0.4$. Using the same parameter values and for QUOTE $= 0$ $S = 0$, the solution to the present problem is computed. It is evident from Fig. 12 that when $S = 0$, our result is in good agreement with Paul [7].

Table 1. Variation of Skin friction τ and Nusselt number Nu with Gr, M, K_p, R, S, a and γ at time $t = 0.6$.

Gr	M	K_p	R	S	a	γ	τ	Nu
3	0.7	0.3	6	5	0.8	0.9	3.9590	1.3405
6	0.7	0.3	6	5	0.8	0.9	3.5574	1.3405
-6	0.7	0.3	6	5	0.8	0.9	5.1637	1.3405
3	**1.7**	0.3	6	5	0.8	0.9	4.3137	1.3405
3	0.7	**0.5**	6	5	0.8	0.9	3.4317	1.3405
3	0.7	0.3	**20**	5	0.8	0.9	4.0894	2.7377
3	0.7	0.3	6	**6.2**	0.8	0.9	3.9339	1.1445
3	0.7	0.3	6	**-3**	0.8	0.9	4.0534	2.2549
3	0.7	0.3	6	**-12**	0.8	0.9	4.1027	2.9471
3	0.7	0.3	6	5	**1.2**	0.9	5.3192	1.3405
3	0.7	0.3	6	5	0.8	**1.4**	4.4734	1.5339
3	0.7	0.3	6	5	0.8	**-0.4**	2.8447	0.9254
3	0.7	0.3	6	5	0.8	**-0.9**	2.5045	0.8005

6. Conclusion

An unsteady MHD natural convective flow of heat and mass transfer over an exponentially accelerated infinite vertical porous plate with heat source, radiation, and suction/injection in a porous medium, has been formulated and resolved analytically by using Laplace transform technique. The important conclusions are:

The occurrence of a transverse magnetic field causes a resistance to the flow velocity, whereas a saturated porous medium improves it.

The accelerating parameter expands the velocity profiles of the fluid.

The outcome of heat source $(S > 0)$ as well as convection current due to cooling of the plate $(Gr > 0)$ is to enhance momentum profiles.

Escalation in the radiation parameter reduces the thermal state of the stream.

Fluid suction increases skin friction, whereas heat source decreases it.

The heat transfer rate is boosted by enhancing suction and radiation, whereas the heat source describes the opposite phenomenon.

References

1. F. Ali, I. Khan, S. Shafie, and N. Musthapa, Heat and Mass Transfer with Free Convection MHD Flow Past a Vertical Plate Embedded in a Porous Medium, *Math. Probl. Eng.*, *2013*, 2013, 1–13. https://doi.org/10.1155/2013/346281.
2. D.A. Nield, and A. Bejan, *Convection in Porous Media* (Cham, Springer International Publishing, 2017). https://doi.org/10.1007/978-3-319-49562-0.
3. H.M. Shawky, N.T.M. Eldabe, K.A. Kamel, and E.A. Abd-Aziz, MHD flow with heat and mass transfer of Williamson nanofluid over stretching sheet through porous medium, *Microsyst Technol.*, *25*, 2019, 1155–1169. https://doi.org/10.1007/s00542-018-4081-1.
4. M.V. Reddy, and P. Lakshminarayana, Higher Order Chemical Reaction and Radiation Effects on Magnetohydrodynamic Flow of a Maxwell Nanofluid With Cattaneo–Christov Heat Flux Model Over a Stretching Sheet in a Porous Medium, *J. Fluids Eng.*, *144*, 2022, 1–9. https://doi.org/10.1115/1.4053250
5. J.R. Pattnaik, G.C. Dash, and S. Singh, Radiation and mass transfer effects on MHD flow through porous medium past an exponentially accelerated inclined plate with variable temperature, *Ain Shams Eng. J.*, *8*, 2017, 67–75. https://doi.org/10.1016/j.asej.2015.08.014.
6. M. Umamaheswar, M.C. Raju, and S.V.K. Varma, Effects of Time Dependent Variable Temperature and Concentration Boundary Layer on MHD Free Convection Flow Past a Vertical Porous Plate in the Presence of Thermal Radiation and Chemical Reaction, *Int. J. Appl. Comput. Math.*, *3*, 2017, 679–692. https://doi.org/10.1007/s40819-015-0124-9.
7. A. Paul, Transient Free Convective MHD Flow Past an Exponentially Accelerated Vertical Porous Plate with Variable Temperature through a Porous Medium, *Int. J. Eng. Math.*, *2017*, 2017, 1–9. https://doi.org/10.1155/2017/2981071.
8. A.O. Ajibade, A.M. Umar, and T.M. Kabir, An analytical study on effects of viscous dissipation and suction/injection on a steady mhd natural convection couette flow of heat generating/absorbing fluid, *Adv. Mech. Eng.*, *13(5)*, 2021, 1–12. https://doi.org/10.1177/16878140211015862.
9. O.D. Makinde, Z.H. Khan, R. Ahmad, R.U. Haq, and W.A. Khan, Unsteady MHD Flow in a Porous Channel with Thermal Radiation and Heat Source/Sink, *Int. J. Appl. Comput. Math.*, *5*, 2019, 1–21. https://doi.org/10.1007/s40819-019-0644-9.
10. N.N. Reddy, V.S. Rao, and B.R. Reddy, Chemical reaction impact on MHD natural convection flow through porous medium past an exponentially stretching sheet in presence of heat source/sink and viscous dissipation, *Case Stud. Therm. Eng.*, *25*, 2021,

1–11. https://doi.org/10.1016/j.csite.2021.100879.

11. S.G. Bejawada, Z.H. Khan, and M. Hamid, Heat generation/absorption on MHD flow of a micropolar fluid over a heated stretching surface in the presence of the boundary parameter, *Heat Transf.*, *50(6)*, 2021, 6129–6147. https://doi.org/https://doi.org/10.1002/htj.22165.
12. K.R. Cramer, and S.I. Pai, *Magnetofluid dynamics for engineers and applied physicists*, (New York, McGraw-Hill Book Company, 1973).
13. H. Schlichting, and K. Gersten, *Boundary-Layer Theory*, (Berlin, Heidelberg, Springer Berlin Heidelberg, 2017). https://doi.org/10.1007/978-3-662-52919-5.
14. A. Paul, and R.K. Deka, Unsteady Natural Convection Flow past an Infinite Cylinder with Thermal and Mass Stratification, *Int. J. Eng. Math.*, *2017*, 2017, 1–13. https://doi.org/10.1155/2017/8410691.
15. R.K. Deka, A. Paul, and A. Chaliha, Transient free convection flow past vertical cylinder with constant heat flux and mass transfer, *Ain Shams Eng. J.*, *8*, 2017, 643–651. https://doi.org/10.1016/j.asej.2015.10.006.
16. N.W. McLachlan, *Complex Variable Theory and Transform Calculus: With Technical Applications* (Cambridge, Cambridge University Press, 1955).